TID-4500, UC-35
Nuclear Explosions—
Peaceful Applications

Lawrence Radiation Laboratory
UNIVERSITY OF CALIFORNIA
LIVERMORE

UCRL-50486

FROZEN EARTH MATERIALS AS SEISMIC DECOUPLING MEDIUMS

T. R. Butkovich

August 26, 1968

FROZEN EARTH MATERIALS AS SEISMIC DECOUPLING MEDIUMS

Abstract

The SOC computer code, designed to calculate the effects of detonations of contained explosions on the surrounding medium, was used to calculate a source function called the reduced displacement potential. The input to the code was an experimentally determined equation of state for each of the following frozen earth materials (at -10° C): dry and ice-saturated sand, partially and fully ice-saturated glacial till, and ice. The reduced displaced potential was convolved with the response of the Benioff seismometer and appropriate attenuation operators. The first half-cycle displacement amplitudes at 300 and 500 km were compared to those obtained from particle velocity measurements for nuclear events in four mediums. These results, scaled to 5 kt and normalized to tuff, are: tuff 1, granite 2.43, salt 2.63, and alluvium 0.18, for actual nuclear events; and ice 0.78, 100% saturated sand 0.56, 100% saturated till 0.67, and 57% saturated till 0.33, for simulated nuclear events in these mediums. The latter value for partially saturated till assumed a compressional velocity of 2400 m/sec for the medium. A lower assumed velocity reduces the values.

Introduction

Over the past few years, considerable attention has been focused on the study of seismic signals emanating from underground nuclear explosions. The primary interest in this study has been to obtain an understanding of the attenuation of the signal between its point of origin and recording stations tens to thousands of kilometers away.

It is probably safe to say that the seismic signals have been recorded from every underground nuclear detonation that has taken place. Analyses of these seismic data have shown that the amplitude of the signal of the arrival of the first cycle and a half is dependent on the energy released and the propagation distance between source and station, and is also strongly dependent on the shot environment.[1] Werth, Herbst, and Springer[2] have studied the factors affecting the first arrival of seismic waves from underground nuclear explosions recorded at distances of 96 to 600 km. At these distances, the first seismic signal to arrive is a head wave, a conical wave arising from critical refraction at the Mohorovicic discontinuity. Consequently,

Werth, Herbst, and Springer based their technique on Zvolinskii's head wave theory, which relates the displacement amplitude of the conical wave to a source function called the reduced displacement potential. The reduced displacement potential can be obtained by assuming that the motion near an explosion, but beyond the elastic range r_e, can be represented by the elasticity equation for a spherically symmetric, infinite material. Then a "reduced" displacement potential $A(\tau)$ can be defined by

$$u(r_e, t) = \frac{\partial}{\partial r} \frac{A(\tau)}{r} ,$$

where $\tau = t - r/c$, $u(r_e, t)$ is the displacement, and c is the compressional velocity of the medium. The distant signal is given by $s(\tau) = \theta A(\tau)$, where θ is some operator representing the earth, which corresponds to the impulse response, attenuation, and recording instrument effects.[3]

Werth, Herbst, and Springer[2] have shown that good agreement exists between theory and measurement for several nuclear events in tuff, and in another paper Werth and Herbst[4] have shown that when particle displacement data just beyond the region of inelastic medium response for nuclear events in four mediums are used to calculate the reduced displacement potentials, the resultant amplitudes scaled to 5 kt and normalized to tuff are: tuff 1, alluvium 0.25, granite 1.11, and salt 1.61—demonstrating the effect of the shot medium.

Computer codes developed at Lawrence Radiation Laboratory have been used to calculate, with considerable success, the effects of detonations on the surrounding medium.[5,6] Recently the codes have been improved by the incorporation of a more realistic failure model[7] and better material descriptions.[8,9,10] With adequate material descriptions, obtained in situ and on samples recovered from the shot environment, excellent agreement between experimental measurements and calculations is consistently obtained.[10]

The intense shock generated by an underground nuclear explosion vaporizes, fuses, fractures, and permanently displaces the close-in rock. The outgoing seismic wave is essentially spherical and degenerates from a strong shock wave to an elastic wave. The equation (in finite difference form) relating particle displacement time history at some radius r_e in the elastic region is then used to calculate the reduced displacement potential. The reduced displacement potential can be calculated for any complicated u(t) from outside the inelastic region. As long as no characteristic time or distances are involved, the potential formed from the displacement history of an explosion yield (W_1) may be cube-root scaled to another yield (W_2) in the same medium. The scaling goes as[11]

$$A_2(\tau) = A_1(\tau)\,(W_2/W_1)$$

$$\tau_2 = \tau_1\,(W_2/W_1)^{1/3}$$

The continuing program in the seismic-decoupling studies, funded in part by the Advanced Research Project Agency (ARPA), includes calculations and material properties studies. Previous studies suggest that materials with high dry porosities are good decoupling mediums in that very little energy is transmitted out

of the medium into the seismic wave. Other materials may also be good decoupling mediums because of unique properties, i.e., phase transitions that take place under shock conditions.

Perennially frozen ground, or permafrost, is a common phenomenon which underlies a major portion of the land areas above the arctic circle to depths of as much as 500 m.

Experimental

CHOICE OF MATERIALS

The existence of permafrost is determined by thermal conditions and is essentially independent of the composition of earth materials. Virtually any type of geological material may be perennially frozen. The properties of permafrost are markedly affected by the presence of ice in varying quantaties, which indurates otherwise unconsolidated sediment. Therefore, the natural variability of earth materials associated with varying ice volume makes it difficult to find or make-up a typical material. The samples on which tests were conducted were chosen and made up by the U. S. Army Cold Regions Research and Engineering Laboratory (CRREL).[12] The samples were prepared at varying ice contents and represent a wide range of naturally occurring conditions. The sample materials are (1) Ottawa banding sand, a well rounded, well sorted, quartz sand with a median diameter of 100 μ; (2) West Lebanon glacial till, a multimineralic, very poorly sorted, extremely well graded material with no particle larger than 145 μ and a median diameter of 36 μ; and (3) pure polycrystalline and single crystal ice, the matrix material in permafrost.

ISOTHERMAL COMPRESSIBILITY

The technique used was the same as that described by Stephens.[9] All measurements were made at -10°C (14°F). Figures 1a-e show the isothermal compressibility of Ottawa sand with varying degrees of saturation. Figures 2a and 2b show the data for glacial till at 57% and 100% saturation. Figure 3 shows the compressibility of ice. In each case both the loading and unloading curves are given.

DYNAMIC HUGONIOT MEASUREMENTS

Stanford Research Institute (SRI) made dynamic Hugoniot equation-of-state measurements on samples with the same specifications as those used for the hydrostatic compressibility measurements of CRREL.[13] Table I summarizes the results. All tests were conducted with an initial shot temperature of -10°C.

TRIAXIAL STRENGTH MEASUREMENTS

Triaxial and unconfined compressive strength tests were conducted on four frozen materials: saturated fine-grained sand, saturated and partially

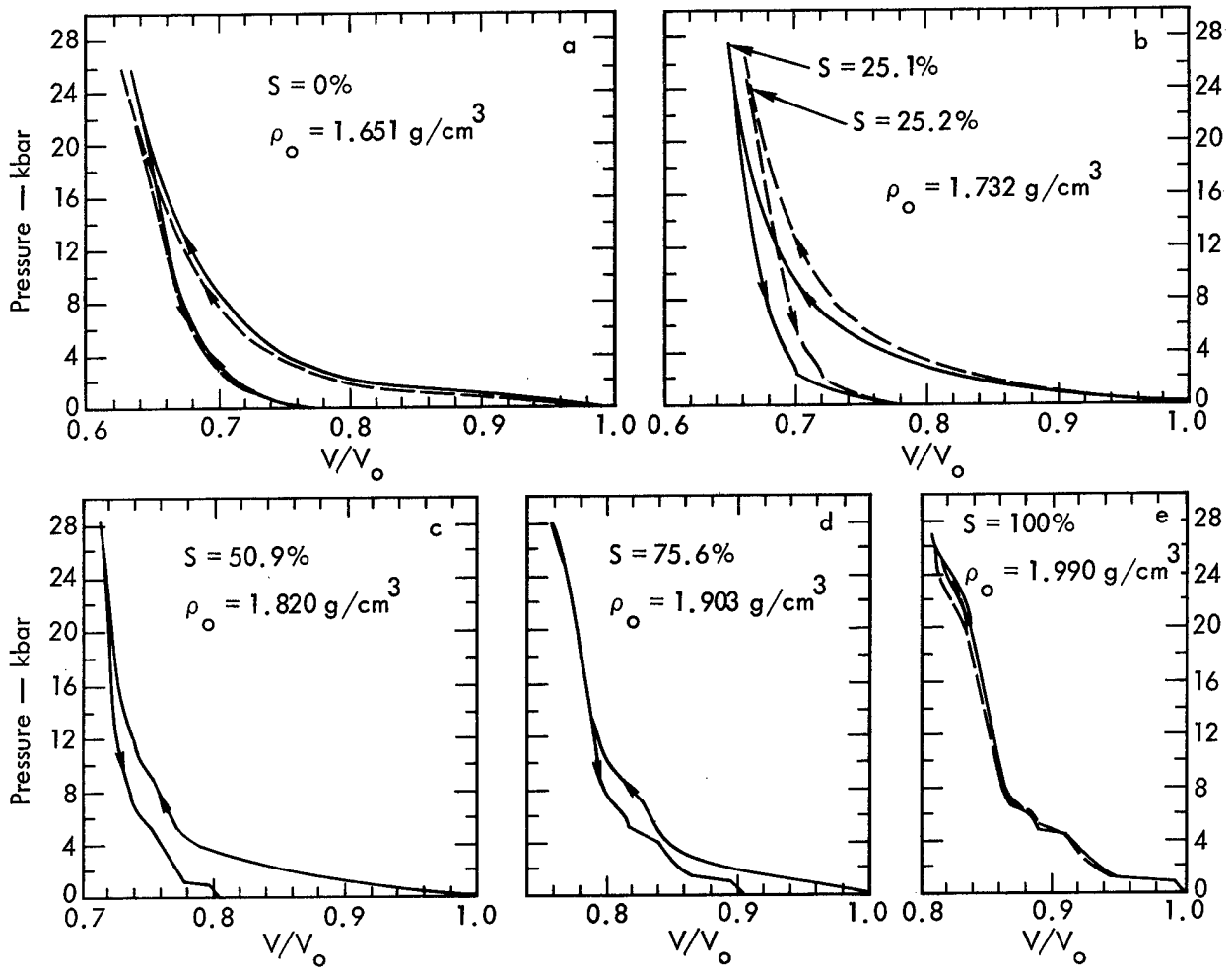

Fig. 1. Isothermal compressibility of frozen Ottawa banding sand at -10°C for five degrees of saturation (S).

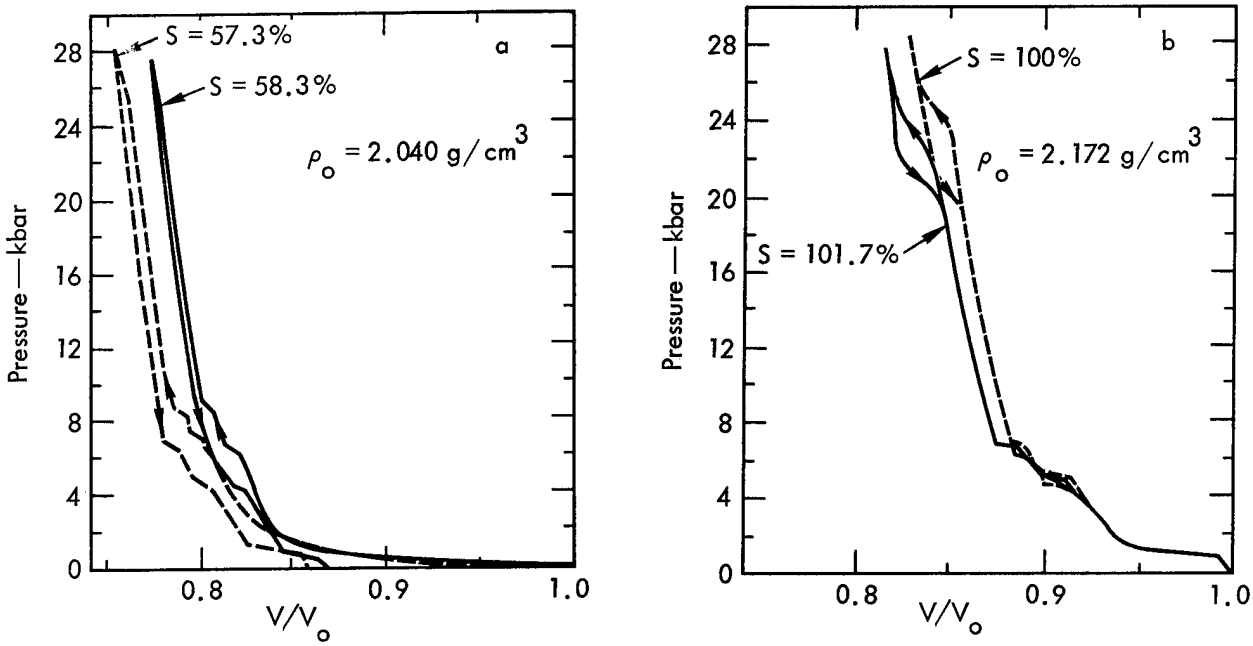

Fig. 2. Isothermal compressibility of frozen West Lebanon glacial till at -10° C for 58% and 100% saturation.

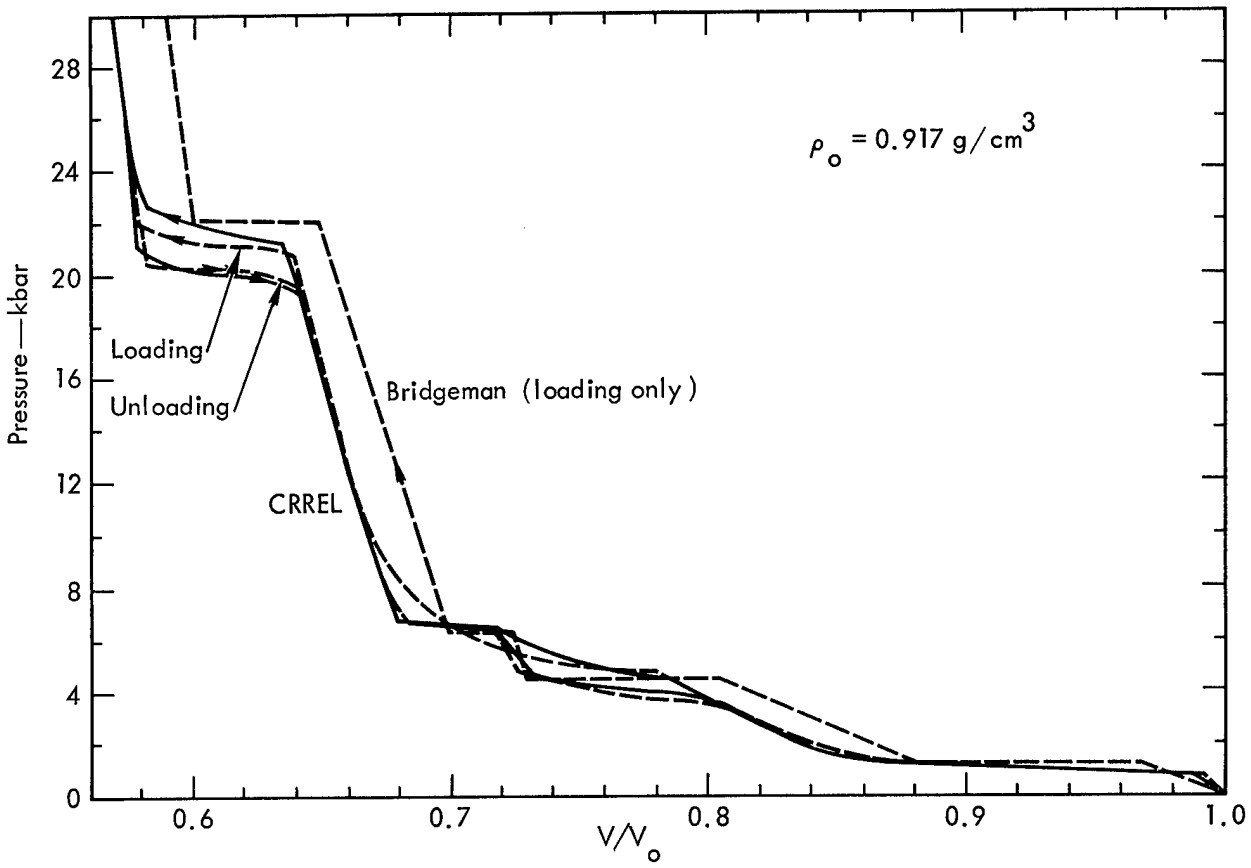

Fig. 3. Isothermal compressibility of polycrystalline ice at -10°C.

Table I. Dynamic Hugoniot equation-of-state measurements by SRI (-10°C).

Material	Shock velocity (cm/μsec)	Particle velocity (cm/μsec)	Pressure (kbar)	Final volume (cm^3/g)
Dry sand ρ_o = 1.65 g/cm^3	0.407	0.217	146	0.2823
	0.405	0.255	150	0.2097
	0.531	0.313	274	0.2486
	0.639	0.381	404	0.2449
Sand (20% sat.) ρ_o = 1.72 g/cm^3	0.298	0.114	58	0.3590
	0.434	0.205	155	0.3071
	0.424	0.212	156	0.2906
	0.539	0.304	282	0.2527
	0.599	0.349	362	0.2428
	0.643	0.374	413	0.2431
Sand (50% sat.) ρ_o = 1.84 g/cm^3	0.340	0.111	69.5	0.3661
	0.466	0.198	170	0.3127
	0.532	0.279	273	0.2584
	0.573	0.308	325	0.2509
	0.637	0.344	403	0.2499

Table I (Continued)

Material	Shock velocity (cm/μsec)	Particle velocity (cm/μsec)	Pressure (kbar)	Final volume (cm^3/g)
Sand (100% sat.) ρ_o = 1.96 g/cm^3	0.377	0.103	76	0.3708
	0.400	0.101	80	0.3813
	0.386	0.105	80	0.3714
	0.510	0.201	201	0.3091
	0.577	0.267	303	0.2736
	0.563	0.271	300	0.2646
	0.596	0.285	339	0.2632
	0.674	0.324	429	0.2649
	0.677	0.331	440	0.2603
	0.704	0.352	487	0.2550
West Lebanon glacial till (dry) ρ_o = 1.86 g/cm^3	0.419	0.208	164	0.2695
	0.417	0.216	167	0.2589
	0.562	0.294	308	0.2552
	0.657	0.365	451	0.2393
West Lebanon glacial till (57% sat.) ρ_o = 2.05 g/cm^3	0.359	0.103	76	0.3470
	0.352	0.107	77	0.3347
	0.482	0.190	187	0.2958
	0.472	0.196	191	0.2853
	0.570	0.265	309	0.2610
	0.591	0.263	319	0.2703
	0.605	0.282	354	0.2593
	0.677	0.319	445	0.2581
	0.658	0.329	444	0.2440
	0.707	0.345	499	0.2500
West Lebanon glacial till (100% sat.) ρ_o = 2.145 g/cm^3	0.390	0.100	83	0.3466
	0.525	0.194	218	0.2939
	0.596	0.259	332	0.2636
	0.701	0.311	467	0.2593
	0.754	0.334	542	0.2596
Single-crystal ice ρ_o = 0.917 g/cm^3	0.295	0.130	35.5	0.6081
	0.321	0.125	37.5	0.666
	0.612	0.319	180	0.5212
	0.755	0.394	274	0.5207
Polycrystalline ice ρ_o = 0.917 g/cm^3	0.323	0.125	37.5	0.6687
	0.500	0.230	106	0.5889
	0.672	0.336	207	0.5445
	0.781	0.419	301	0.5055

saturated glacial till, and polycrystalline ice. All tests were conducted at -10°C.[14] For frozen soil the prevailing mode of failure is plastic in nature. In addition to being temperature sensitive, the mode of failure is strain rate sensitive—the frozen soils become more brittle with increasing strain rate. The maximum value of mean stress obtainable was limited by the triaxial apparatus available.

Since the matrix material in frozen soils is ice, strengths are strongly influenced by the properties of the ice matrix. Figure 4 shows the results of measurements on several frozen materials.

SOC CODE CALCULATIONS

In the measurement program, effectively nine different materials were tested, when one considers that each saturation is a different material. For this study, five materials were chosen as representative of the behavior of permafrost. These are (1) dry sand, which has very large shear strength under high average stresses and no strength at zero average stress; (2) 100% saturated sand; (3) 57% saturated glacial till; (4) 100% saturated glacial till; and (5) the matrix material, ice. The calculations assumed that a 5-kt nuclear detonation had taken place in a homogeneous infinite medium at a depth of burst of 400 $W^{1/3}$ ft (684 ft). In addition, a 5-kt calculation was made for ice at 800 $W^{1/3}$ depth of burst. The equations of state for the five materials were constructed from the experimental data for those materials.

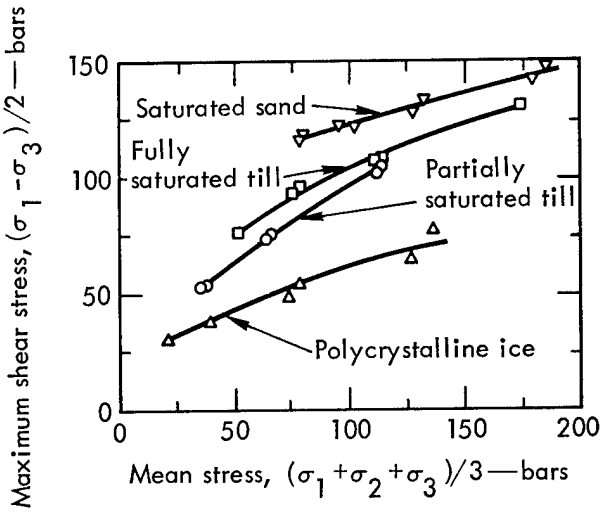

Fig. 4. Triaxial shear strength for several frozen materials at -10°C.

Figures 5, 6, 7, 8 and 9 are the P-V curves used for dry sand, 100% saturated sand, 57% saturated glacial till, 100% saturated glacial till, and ice respectively. The lower parts of the curves, up to 28 kbar, are identical to those shown in Figs. 1, 2, and 3, including all the phase transitions and the unloading curves.

Figures 10a-e show the shear strength versus mean stress relationships used in the calculations. The points are identical to those shown in Fig. 4.

Table II shows various values used in the calculation. ρ_o is the bulk density, k is the elastic bulk modulus, and v_e is the elastic compressional velocity (m/sec). P_1 and P_2 are the limits of mean stress, where it was assumed the materials behaved brittley; above P_2 the material was assumed to be plastic. K_{max} is the maximum allowable shear strength after brittle failure; B is the slope of the maximum shear strength versus mean stress curve after brittle failure, where $K \le BP \le K_{max}$; and σ_{elas} and σ_{failed} are the Poisson's ratios before and after failure respectively.

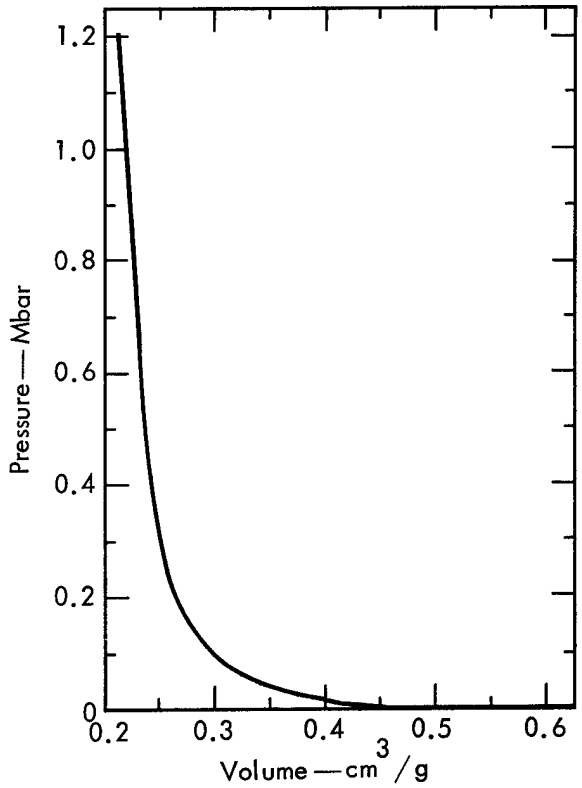

Fig. 5. Hugoniot equation of state for dry Ottawa sand at -10°C.

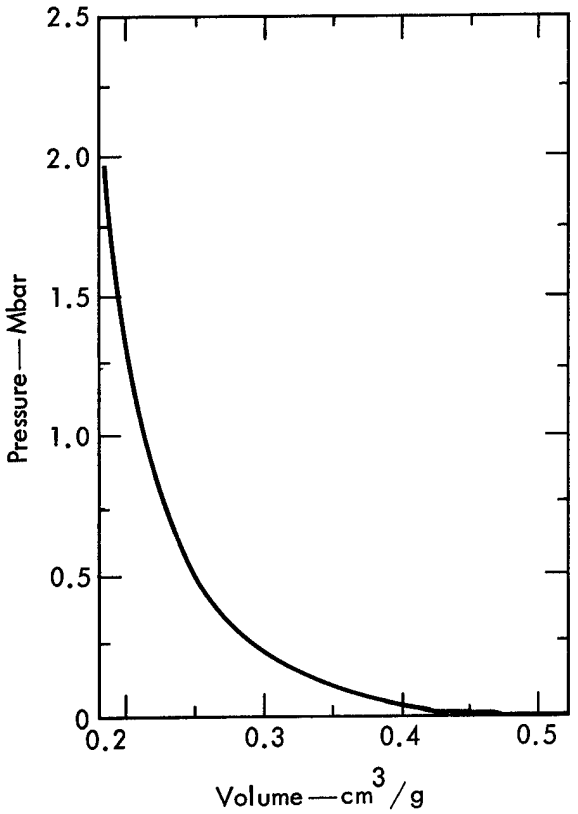

Fig. 6. Hugoniot equation of state for 100% saturated Ottawa sand at -10°C.

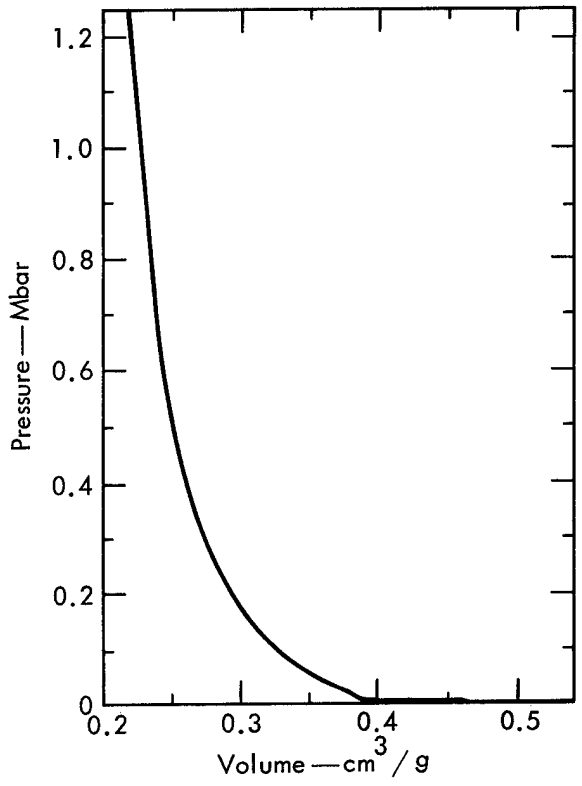

Fig. 7. Hugoniot equation of state for 57% saturated glacial till at -10°C.

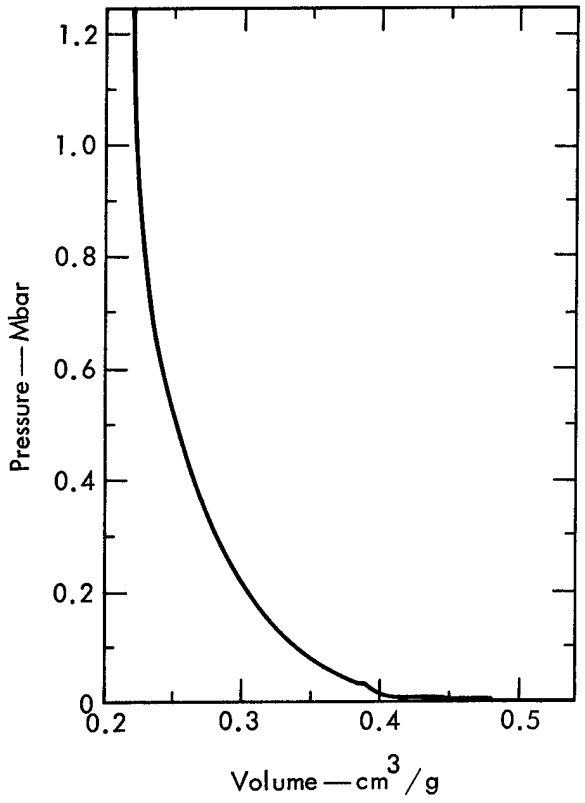

Fig. 8. Hugoniot equation of state for 100% saturated glacial till at -10°C.

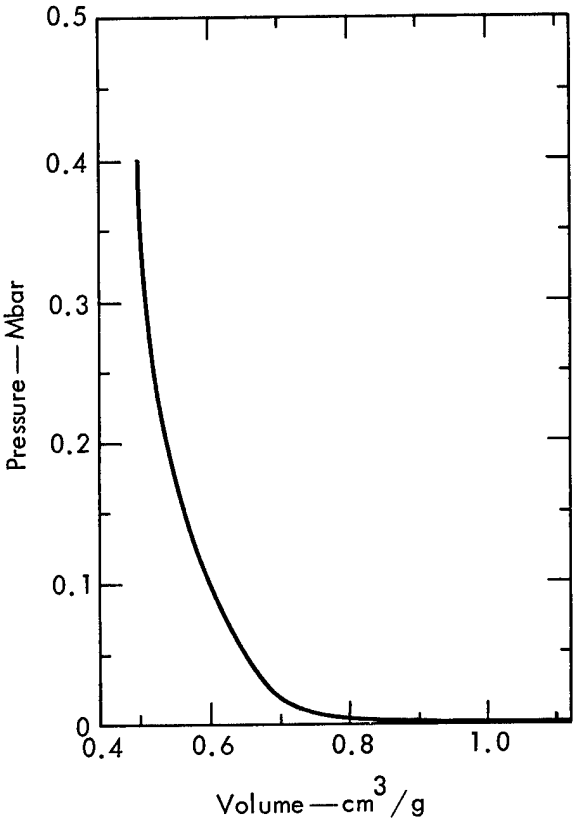

Fig. 9. Hugoniot equation of state for polycrystalline ice at -10°C.

The values of bulk modulus k and elastic velocity v_e were determined either from handbook values (dry sand and ice) or from the initial slope of the isothermal compressibility curve, using the elastic equations

$$(v_e)^2 \rho_o = k + \frac{4}{3}\mu,$$

where μ is the elastic shear modulus, and

$$\mu = 3k\left(\frac{1 - 2\sigma}{2 + 2\sigma}\right).$$

For the 57% saturated till, a velocity of 350 m/sec is obtained from the isothermal compressibility curve to 125 bars, with an assumed Poisson's ratio of 0.35. The fact that the 100% saturated till gives a velocity of 3500 m/sec, makes it difficult to believe that a factor-of-10 difference in velocity occurs between these two saturations; consequently an additional calculation was made using a reported value of 2400 m/sec.[15]

RESULTS OF CALCULATIONS

Table III lists some of the results of the six calculations made on five materials. Two calculations were made on ice to test the effect of depth of burst on the various calculated quantities.

The results indicate that, in general, the static state reduced displacement potential, is related directly to the cavity radius. The steady state reduced displacement potential is not given for dry sand. Dry sand was not allowed to undergo brittle failure, and continues to yield

Table II. Parameters used in SOC code calculations.

	ρ_o (g/cm³)	k (kbar)	v_e (m/sec)	P_1 (kbar)	P_2 (kbar)	K_{max} (kbar)	B	σ_{elas}	σ_{failed}
Dry sand	1.65	7.09	833	0	0	6	0.5	0.3	0.3
100% saturated sand	1.985	107.09	2800	0	0.05	0.2	0.75	0.35	0.35
57% saturated till	2.03	1.72 80.95	350 2400	0	0.05	0.16	0.7	0.35	0.35
Ice	0.917		3600	0	0.2	0.16	0.4	0.35	0.35

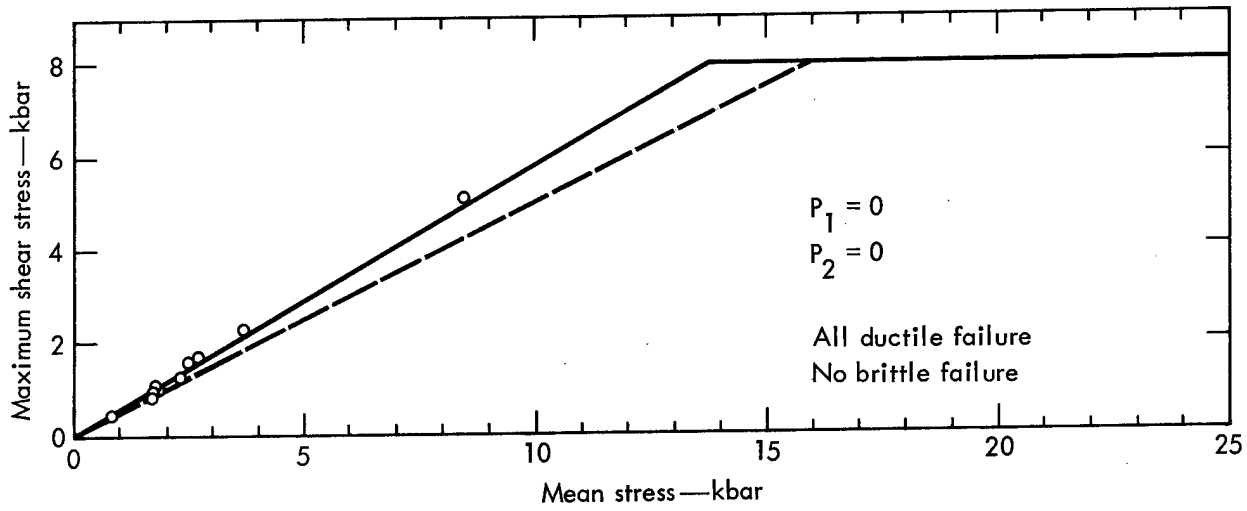

Fig. 10a. Triaxial shear strength versus mean stress for dry Ottawa sand at -10°C.

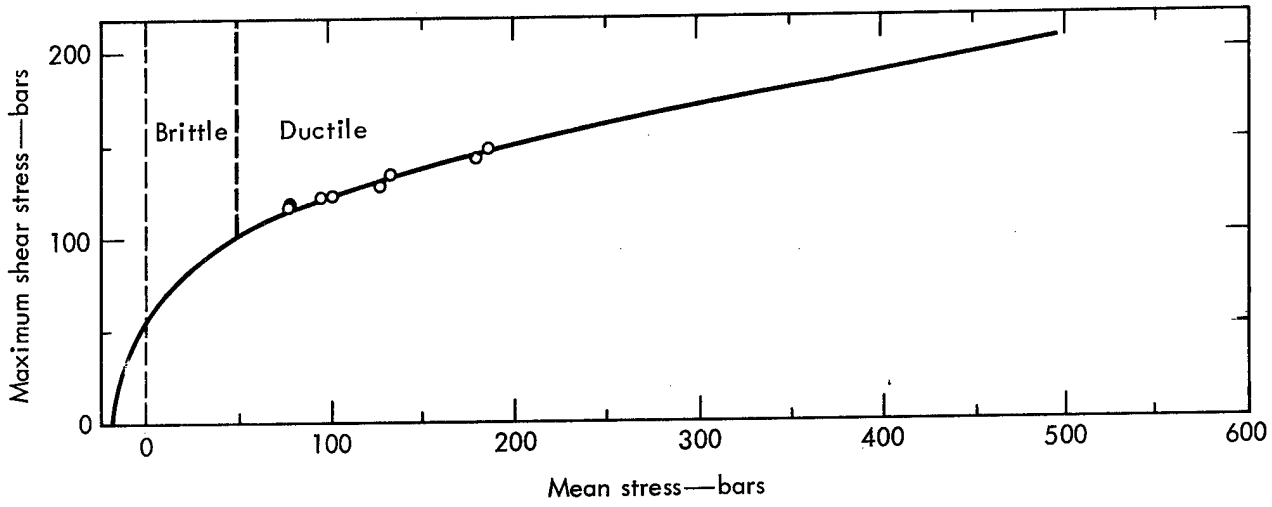

Fig. 10b. Triaxial shear strength versus mean stress for 100% saturated sand at -10°C.

plastically to zero mean stress. Consequently the calculated reduced displacement potential for dry sand continues to decrease with distance. The reduced displacement potential is a strong function of the porosity of the medium. For a partially saturated material with dry porosity like the till, the reduced displacement potential is not meaningful except for that particular saturation.

Figure 11 shows the calculated peak particle velocity versus distance for the five materials at overburden (ρgh) pressures of the 208-m depth of burst.

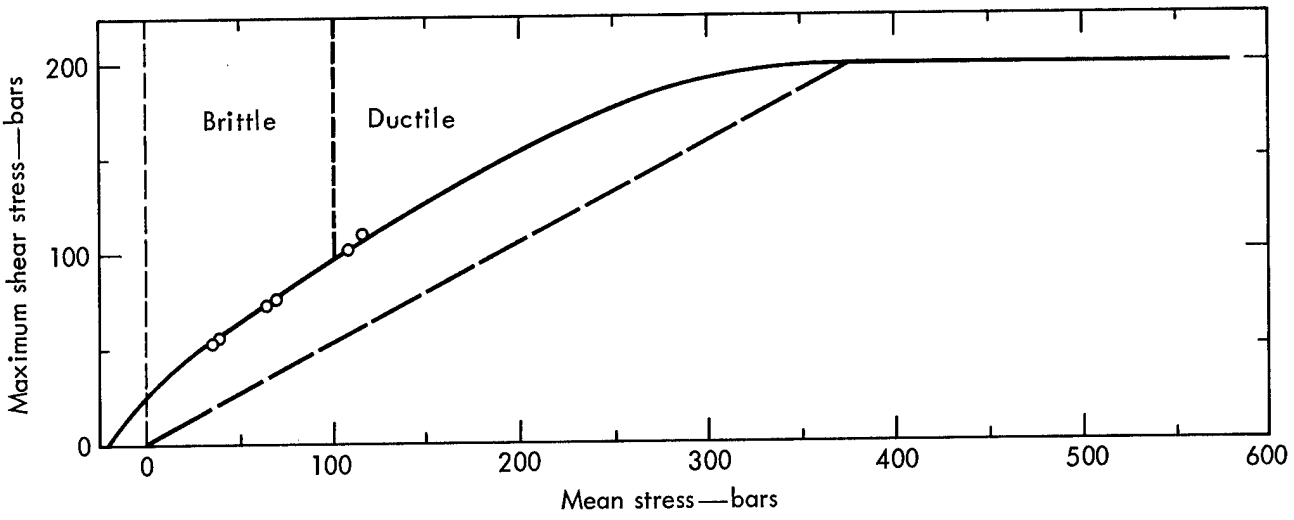

Fig. 10c. Triaxial sheet strength versus mean stress for 57% saturated glacial till at -10°C.

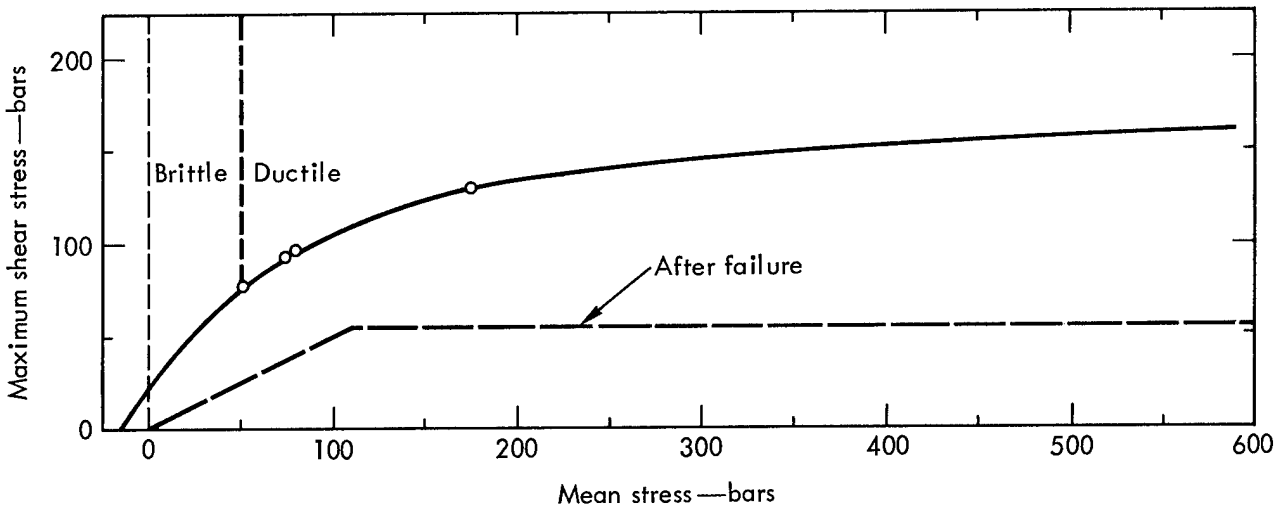

Fig. 10d. Triaxial sheet strength versus mean stress for 100% saturated glacial till at -10°C.

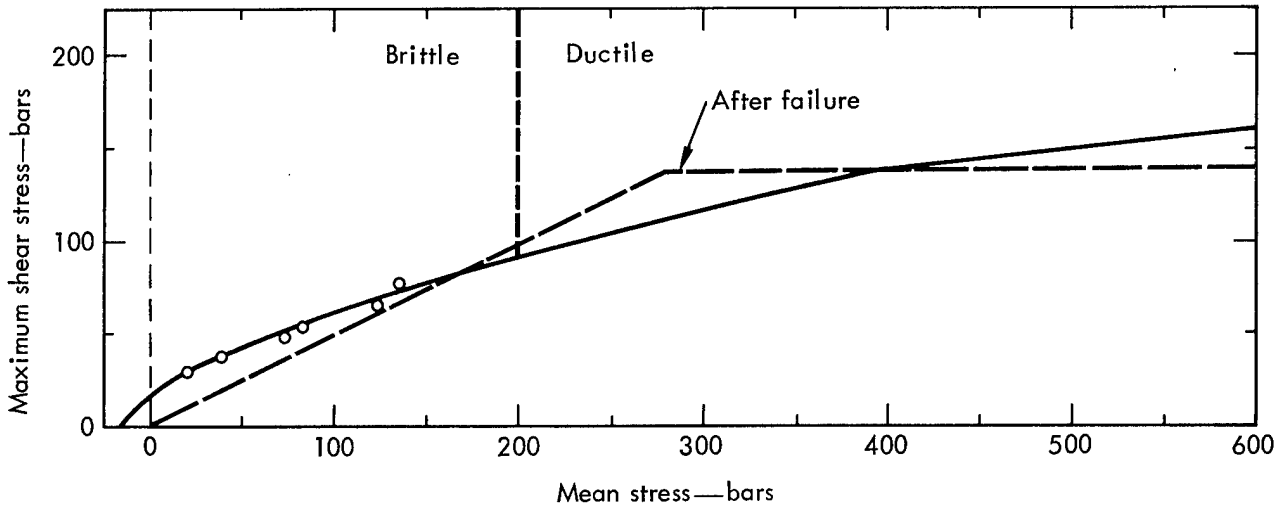

Fig. 10e. Triaxial shear strength versus mean stress for polycrystalline ice at -10°C.

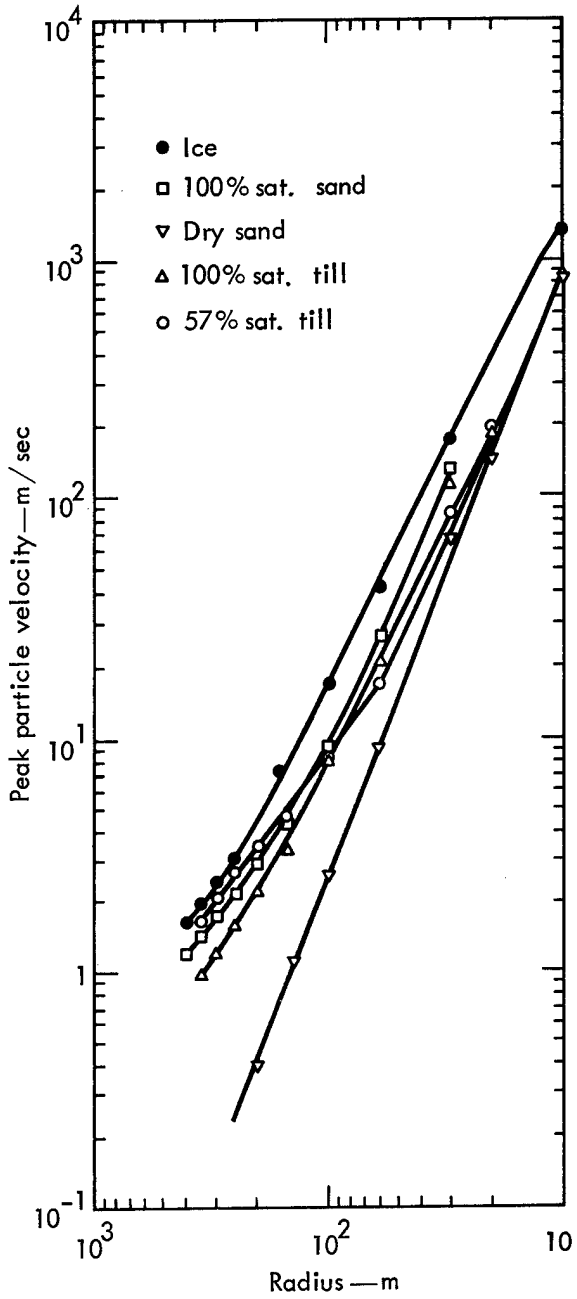

Fig. 11. Calculated peak particle velocity as a function of distance for the five materials studied (DOB = 208 m).

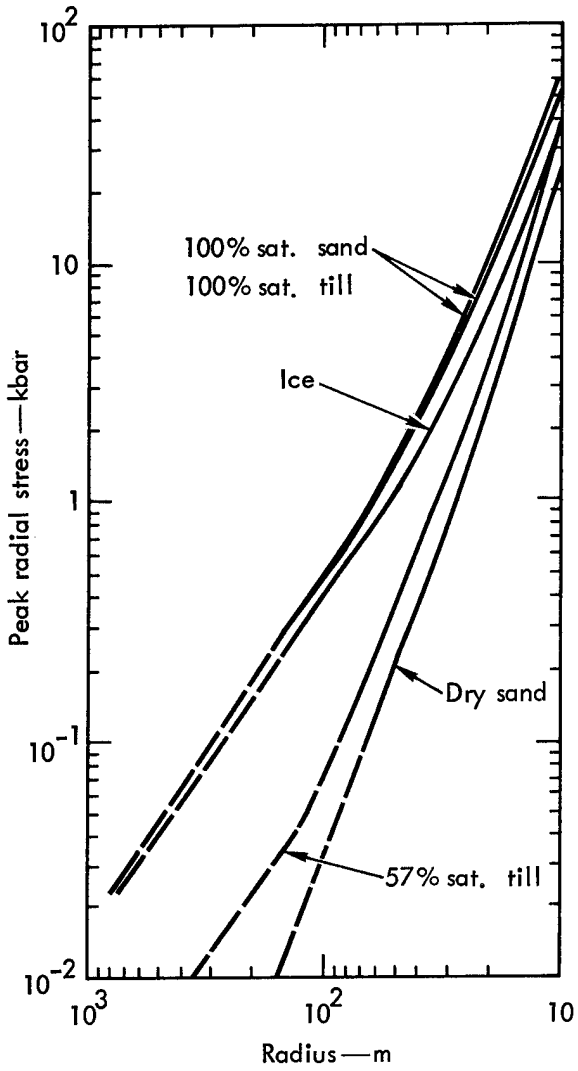

Fig. 12. Calculated peak radial stress as a function of distance for the five materials studied (with overburden subtracted out) (DOB = 208 m).

Figure 12 shows the peak radial stress as a function of distance for the same calculations. Figure 13 shows the radial stress pulse shape at 30 m for each calculation. Figure 14 shows the reduced displacement potential for those calculations reported in Table III at 208-m depth of burst. The calculation made with ice at 416-m depth of burst shows the effect of depth of burst on the reduced displacement potential.

ANALYSIS OF RESULTS

The analysis made is based on a comparison of the calculated first half-cycle displacement as reported by Werth and Herbst.[4] They calculated reduced displacement potential from particle

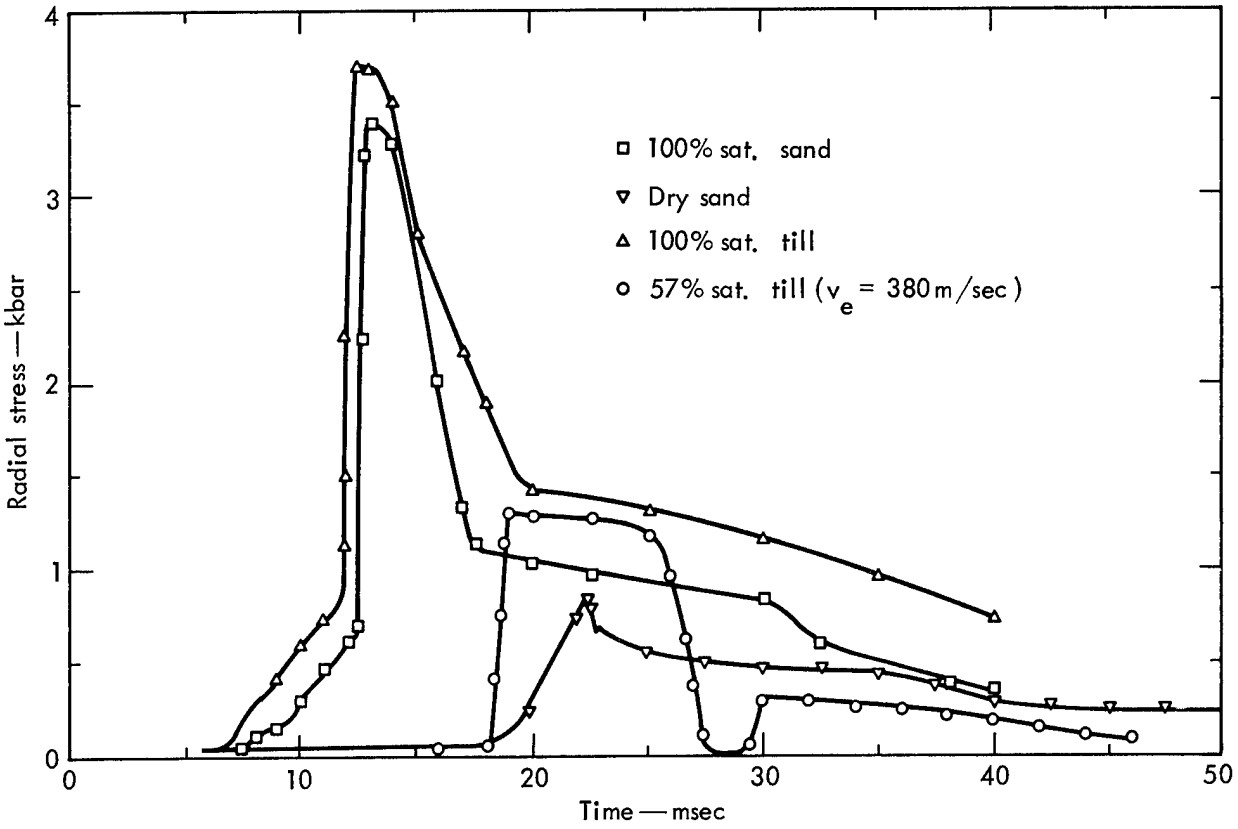

Fig. 13. Calculated radial stress pulse shapes for 5-kt detonations in four frozen earth materials at 30 m from working point (DOB = 208 m).

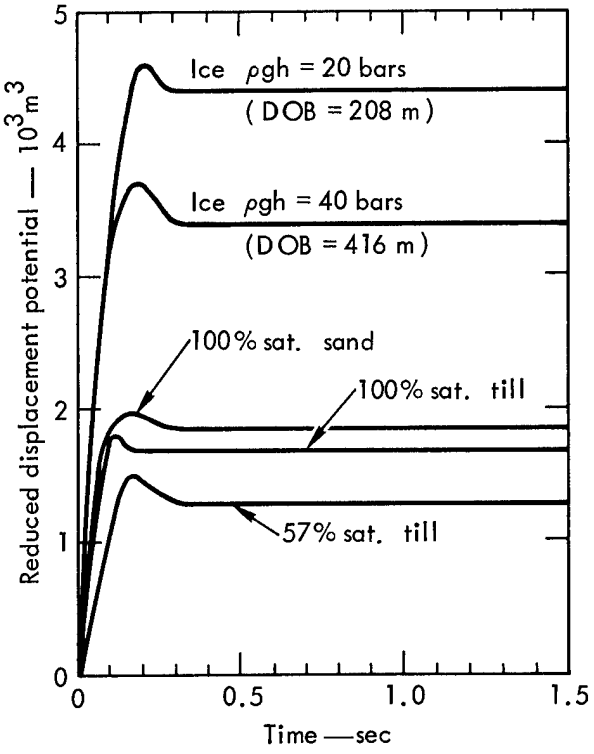

Fig. 14. Calculated reduced displacement potentials for four different media.

velocity measurements just beyond the region of plastic deformations for nuclear explosions in four mediums. The results were scaled to 5 kt and the potentials were convolved with the response of the Benioff instrument with an appropriate attenuation operator. The models of the earth were developed for each explosion, and the results were scaled to tuff as shown in Table IV.

Roberts[16] calculated first half-cycle displacements versus distance for each reduced displacement potential shown in Fig. 13. He used the values of density, and compressional and shear velocity shown in Table III, and the crustal model for the Nevada Test Site. Table V gives the results of these calculations.

With these values, a direct comparison with the four nuclear explosive

Table III. Results of SOC code calculations.

Material	Final cavity radius (m)	Radius of brittle failure (m)	Steady state RDP[a] (m^3)	Overburden pressure (bars)	Equivalent depth of burst (m)
Dry sand	23.96	—	—	34	208 (684 ft)
100% sat. sand	20.12	156.7	1880	40	208
57% sat. till	29.88	76.1	—	41	208
100% sat. till	19.41	252.5	1680	44	208
Ice	26.53	268.2	4300	20	208
Ice	23.95	206.0	3100	40	416 (1368 ft)

[a]Reduced displacement potential.

Table IV. Five-kiloton source with attenuation and crustal models (after Werth and Herbst).[4]

	Tuff	Alluvium	Granite	Salt
First half-cycle amplitude at 300 km	92 mμ	16 mμ	224 mμ	242 mμ
Ratio to tuff	1	0.17	2.43	2.63
First half-cycle amplitude at 500 km	19 mμ	3.5 mμ	43 mμ	40 mμ
Ratio to tuff	1	0.18	2.26	2.11

Table V. Five-kiloton source with attenuation and crustal models.

	First half-cycle amplitude (mμ)					
	Glacial till			Sand	Ice	
Distance (km)	57% sat. v_e = 350 m/sec	57% sat. v_e = 2400 m/sec	100% sat.	100% sat.	ρgh = 40 bars	ρgh = 20 bars
200	15.9	95.7	197.5	163.8	199.6	2218
300	5.1	30.7	61.5	51.4	62.6	71.6
400	2.2	13.2	25.7	21.6	26.9	30.8
500	1.1	6.8	13.0	11.0	13.6	15.9
600	0.6	3.8	7.2	6.1	7.7	9.0
700	0.4	2.4	4.4	3.7	4.7	5.6

mediums used by Werth and Herbst was made. Table VI shows the results.

The above results seem to indicate that saturated frozen earth materials are poorer decoupling mediums than Nevada Test Site valley alluvium. An interesting result is that the assumed low velocity for partially saturated glacial till produces appreciably lower amplitudes. This is due to low compressional wave

Table VI. Resultant amplitudes from Table V normalized to tuff.

		Amplitudes (mμ)					
		Glacial till			Sand	Ice	
	Tuff	57% sat. v_e = 350 m/sec	57% sat. v_e = 2400 m/sec	100% sat.	100% sat.	ρgh = 40 bars	ρgh = 20 bars
First half-cycle amplitude at 300 km	92	5.1	30.7	61.6	51.4	62.6	71.6
Ratio to tuff	1	0.06	0.33	0.67	0.56	0.68	0.78
First half-cycle amplitude at 500 km	19	1.1	6.8	13.0	11.0	13.6	15.9
Ratio to tuff	1	0.06	0.36	0.68	0.58	0.72	0.84

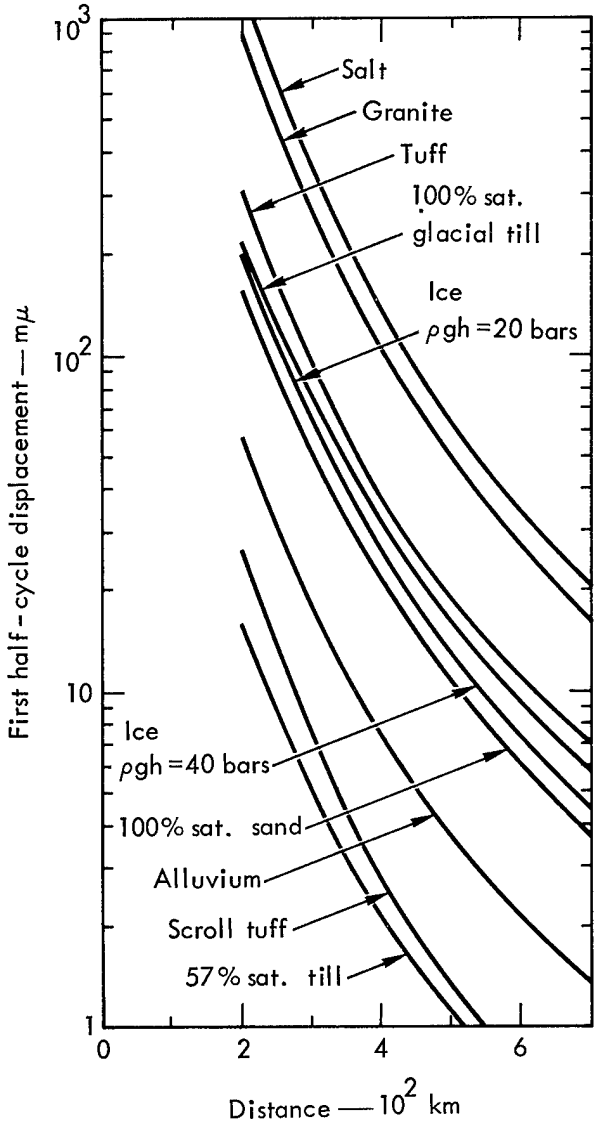

velocity, which leads to an unusually low coupling of the seismic energy out of the detonation medium. Another interesting result shown in Table VI shows the effect of depth of burst on the predicted amplitude.

With regard to the possible low coupling of partially saturated glacial till, it is very unlikely that partially saturated material will be found at containment depths because of the plastic-viscous nature of the matrix material (ice). Because of its ductile nature, loose dry sand could prove to be an excellent decoupling medium, provided it could be found at a sufficient depth and thickness.

Figure 15 shows a comparison of calculated first half-cycle amplitudes (versus distance) of the frozen materials with those reported by Werth and Herbst.[4]

Fig. 15. Comparison of calculated first half-cycle displacement versus distance for several real materials and several hypothetical materials. Displacements are normalized to 5-kt. (Salt —Gnome Event; granite—Hardhat Event; tuff—Rainier Event; alluvium—Fisher Event.)

References

1. D. L. Springer, "Calculation of the First-Zone P Wave Amplitudes for Salmon Event and for Decoupled Sources," J. Geophys. Res. 71, 3459 (1966).
2. G. C. Werth, R. F. Herbst, and D. L. Springer, "Amplitudes of Seismic Arrivals from the M Discontinuity," J. Geophys. Res. 67, 1587 (1962).
3. R. F. Herbst, G. C. Werth, and D. L. Springer, "Use of Large Cavities to Reduce Seismic Waves from Underground Explosions," J. Geophys. Res. 66, 959 (1961).
4. G. C. Werth and R. F. Herbst, "Comparison of Amplitudes of Seismic Waves from Nuclear Explosions in Four Mediums," J. Geophys. Res. 68, 1463 (1963).
5. T. R. Butkovich, "Calculation of the Shock Wave from an Underground Nuclear Explosion in Granite," J. Geophys. Res. 70, 885 (1965).
6. L. Rogers, "Free-Field Motion Near a Nuclear Explosion in Salt: Project Salmon," J. Geophys. Res. 71, 3415 (1966).
7. J. T. Cherry, "Computer Calculations of Explosion-Produced Craters," Int. J. Rock Mech. Min. Sci. 4, 1 (1967).
8. T. R. Butkovich, The Gas Equation of State of Natural Materials, Lawrence Radiation Laboratory, Livermore, Rept. UCRL-14729 (1967).
9. D. R. Stephens, "The Hydrostatic Compression of Eight Rocks," J. Geophys. Res. 69, 2697 (1964).
10. J. T. Cherry, D. B. Larson, and E. G. Rapp, A Unique Description of the Failure of a Brittle Material, Lawrence Radiation Laboratory, Livermore, Rept. UCRL-70617 Preprint (1967), to be published in Int. J. Rock Mech. Min. Sci., 1968.
11. D. W. Patterson, "Nuclear Coupling, Full and Partial," J. Geophys. Res. 71, 3427 (1966).
12. P. Hoekstra and E. Chamberlain, Isothermal Compressibility of Frozen Earth Materials, Army Cold Regions Research and Engineering Lab., Hanover, N. H., Interim Technical Rept. (Oct. 1967).
13. G. D. Anderson, The Equation of State of Ice and Composite Frozen Material, Army Cold Regions Research and Engineering Lab., Hanover, N. H., Research Rept. 257 (1968).
14. E. Chamberlain, Some Triaxial Shear Strength Tests on Frozen Soil and Ice, Army Cold Regions Research and Engineering Lab., Hanover, N. H., Interim Technical Rept. (1967).
15. Hugoniots and Dynamic Properties of Frozen Earth Materials, Final Report (ARPA Order 968), Army Cold Regions Research and Engineering Lab., Hanover, N. H. (July 1967).
16. J. Roberts, Lawrence Radiation Laboratory, Livermore, private communication (1968).

Distribution

LRL Internal Distribution

Michael M. May/D. Sewell	
T. R. Butkovich	25
J. T. Cherry	
M. D. Denny	
L. S. Germain	
A. Holzer	
G. H. Higgins	
J. B. Knox	
M. D. Nordyke	
H. L. Reynolds	
J. E. Roberts	
H. C. Rodean	
D. L. Springer	
P. Stevenson/W. Nervik	
H. A. Tewes	
G. C. Werth	
C. E. Williams/P. Coyle	
TID Berkeley	
TID File	30

External Distribution

R. Black S. Lukasik V. Fryklund Advanced Research Project Agency Washington, D. C.	3
K. King Geodetic Survey Las Vegas, Nevada	3
J. E. Reeves Nevada Operations Office Las Vegas, Nevada	10
A. Garner Division of Military Application Washington, D. C.	3

E. C. Shute
San Francisco Operations Office
Berkeley, California

3

E. Chamberlain
A. Assur
U. S. Army Terrestrial Science Center
Hanover, New Hampshire

TID-4500 Distribution, UC-35, Nuclear Explosions—
Peaceful Applications

255

Printed in USA. Available from the Clearinghouse for Federal Scientific and Technical Information, National Bureau of Standards, U. S. Department of Commerce, Springfield, Virginia 22151
Price: Printed Copy $3.00; Microfiche $0.65.

CRS/rd